Experimental Enhancement of Mixed Convection Heat transfer in Hot Base Rectangular Channel

Experimental Enhancement of Mixed Convection Heat transfer in Hot Base Rectangular Channel

S F Dakhil[1], AQ Najim[1] and FA Abood[2]
[1]Engineering Technical College –Basra, Southern Technical University
[2]Engineering College –Basra, Basrah University.

***Abstract*:** This paper presents an experimental study to enhance the flow and heat transfer enhancement over horizontal and orientation channel with hot base by laminar mixed convection heat transfer. The hot base is fitted with the longitudinal rectangular fin arrays as a finned wall. The study covered the following range: modified Grashof number varied (3×10^8 - 8×10^8), Reynolds number in range 1800-2300, and Pyrantel number 0.71. The bottom finned wall of the channel was supplied with constant heat flux, while the other sides are insulated. The experiment part includes a suitable test rig that was built to get accurate decisions. A good mechanism was created to get the orientation angles at (90°,120°, $150^\circ$and 180°) then to analysis this effect on heat transfer for laminar flow force convection. Three different cases are investigated: the effect of modified Grashof number and orientation angles on fluid particles flow and heat removal will be an enhancement. The experiment results show that the average heat transfer coefficient increased with Reynolds number and an increase of the Grashof number for all orientation angles due to increases buoyancy forces, thus causes a detach with the secondary layer flow. The average heat transfer coefficient and fins effectiveness are enhanced to 25% at highest longitudinal orientation angles.

Keywords: Internal flow-Mixed-Laminar-Arrayfins- Orientental channel.

1. Introduction

In the actual application for hot base channelled, the generated heat is not dissipating rapidly to its surrounding atmosphere, this may cause a rise in temperature of the system components. This byproduct causes serious overheating problems in the system and leads to system failure, so the heat generates by the system must be removed to its surrounding to provide the system at standard thermal condition [1]. Electrical applications: Cooling of electronic equipment.g.cooling Personal Computers, LED, high power chip, and projector. Mechanical applications: air conditioning equipment, Automobile vehicles. There are different methods to enhancement heat transfer depended on the application and required work (cooling/heating) such as increase area by adding fins or different shape cavities, Nanofluid, swirl etc [3]. Heat transfer enhancement can be categorized as passive cooling techniques or active cooling techniques depended on enhances methods used in the application. Passive techniques enhanced by additional surface geometries, or fluid additives. While active techniques need external power, such as electric or acoustic fields and moving boundary layer as mentioned in Table 1. All industrial applications, increase surface area such as fins heat sink and shape of cavities are one of the most inexpensive and common ways to dissipate unwanted heat by the rotation of duct, use of Nanofluid etc, to guarantee the thermal design of the system is optimized [3,4]. This work includes studying the effect

of surface area that includes fins, the effect of orientation of the duct and studies the shape modifications as improvement methods on heat transfer and fluid flow.

Table 1. TheEnhancement Techniques[3,4].

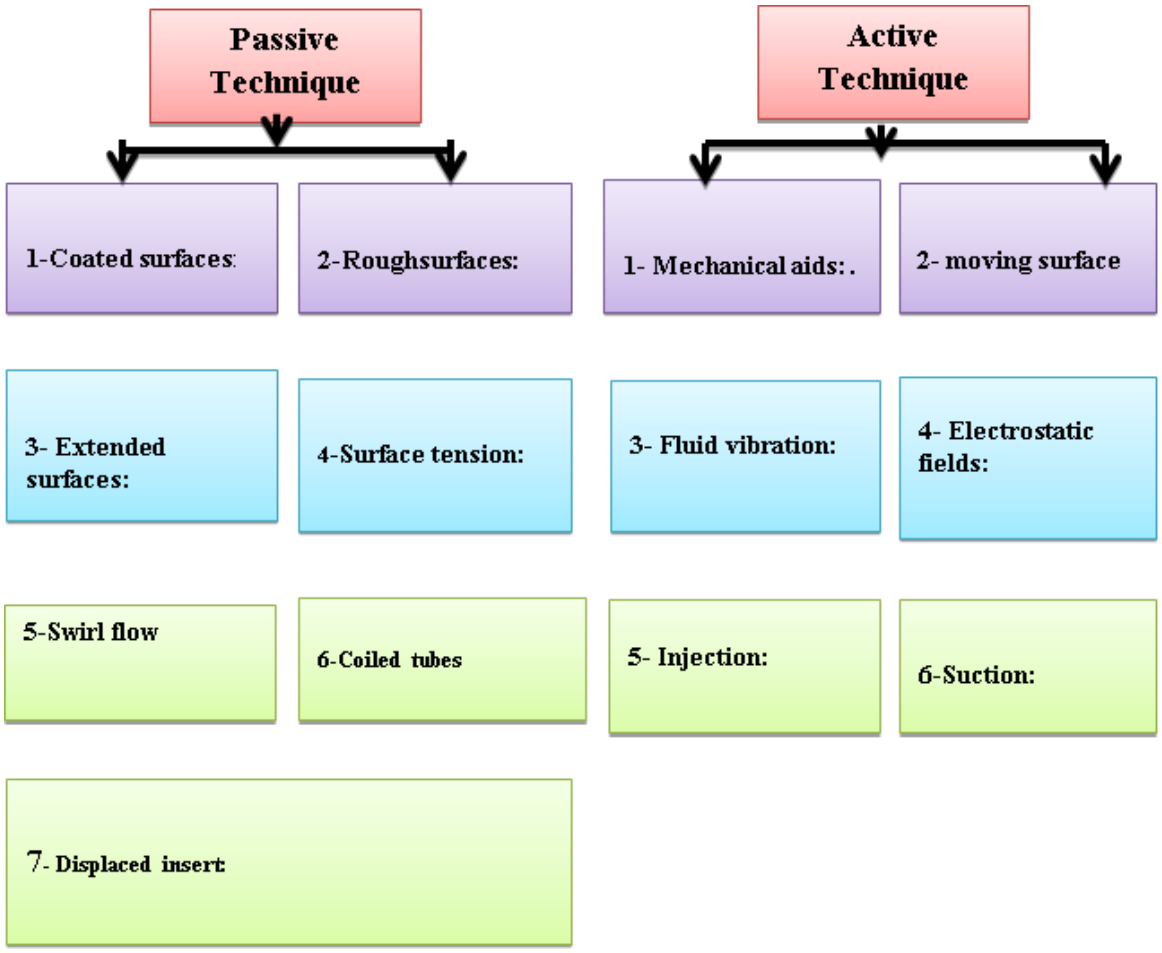

2. Main Components of the Rig

The test rig comprises of the main components as Wind Tunnel, Test section, Heat circuit, Centrifugal fan. The details of each component are explained in the next sections:

2.1 General Description of Wind Tunnel

A schematic drawing of the experimental work is shown in Fig 1. The main part of the experimental rig consists of a horizontal channel with 150 cm long, 30 cm width and 10 cm height. The bottom surface is exposed to heat flux while the other surface isolated. This duct divided into three regions, first region unheated entrance which made of (60) cm long then test section made of (60) cm long with (15) rectangular fins while the end of duct made of (30) cm long unheated region. A wind tunnel which is consists of nozzle (20) cm long and damping chamber (20×30×50) cm, it is used to reduce the flow fluctuations and to get a uniform flow at the test section. While the ending region of the channel connected to the nozzle with 30 cm long this nozzle connected to the AC fan by a flexible hose. The air velocity is measured by a flow meter located at the end of the test section. The inlet temperature of the air is measure by Infrared Thermometerwhile outlet temperature measured by one thermocouple fixed with pitot tube that located in outside air from nozzle.

2.2 Test section

The actual photo of the test rig consists of a heating plate with of rectangular duct with (60) cm long, (30) cm width and (0.6) cm thick aluminium, finned wall plate with (15) longitudinal fins fixed on the plate, besides of a heater plate and thermocouples. The aluminium fins array of (2) mm thick, (60) mm height and (60) cm length were welded to the plate by machining longitudinal slots (2) mm width and (3) mm depth. The test section was presented with a special insulator, of (15) cm on all side to insulate the section from the ambient and to drive all heat to fins.

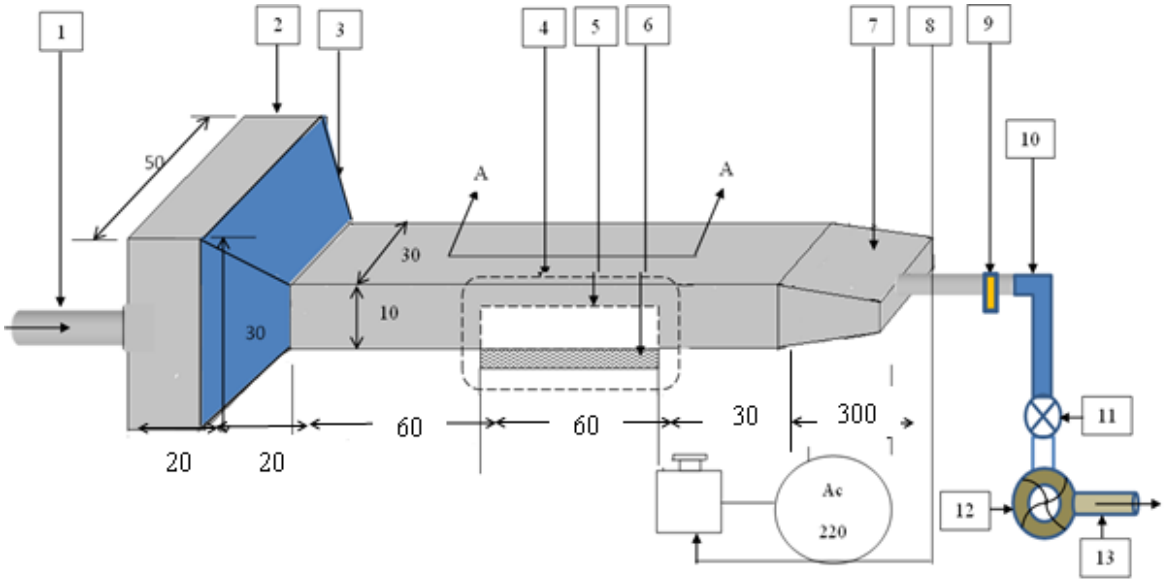

Figure 1. Schematic diagram of the present work rig, dimensions in cm; 1- Inlet air 2- Damping Chamber 3- Inlet Nozzle4- Test section 5- Fin 6-Surface Heat Source 7- Out Nozzle 8- Variac9- air flowmeter 10- flexible hose11- valve 12- fan 13- air outlet

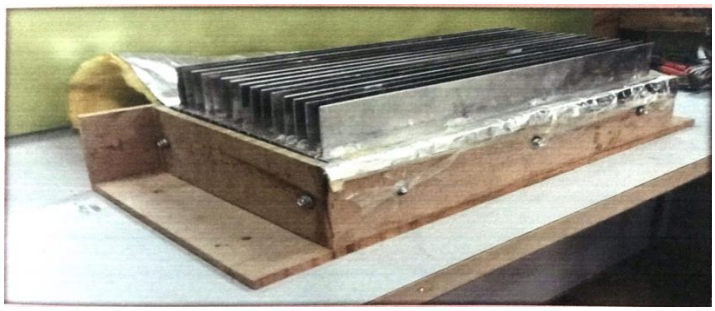

Figure 2. The test section

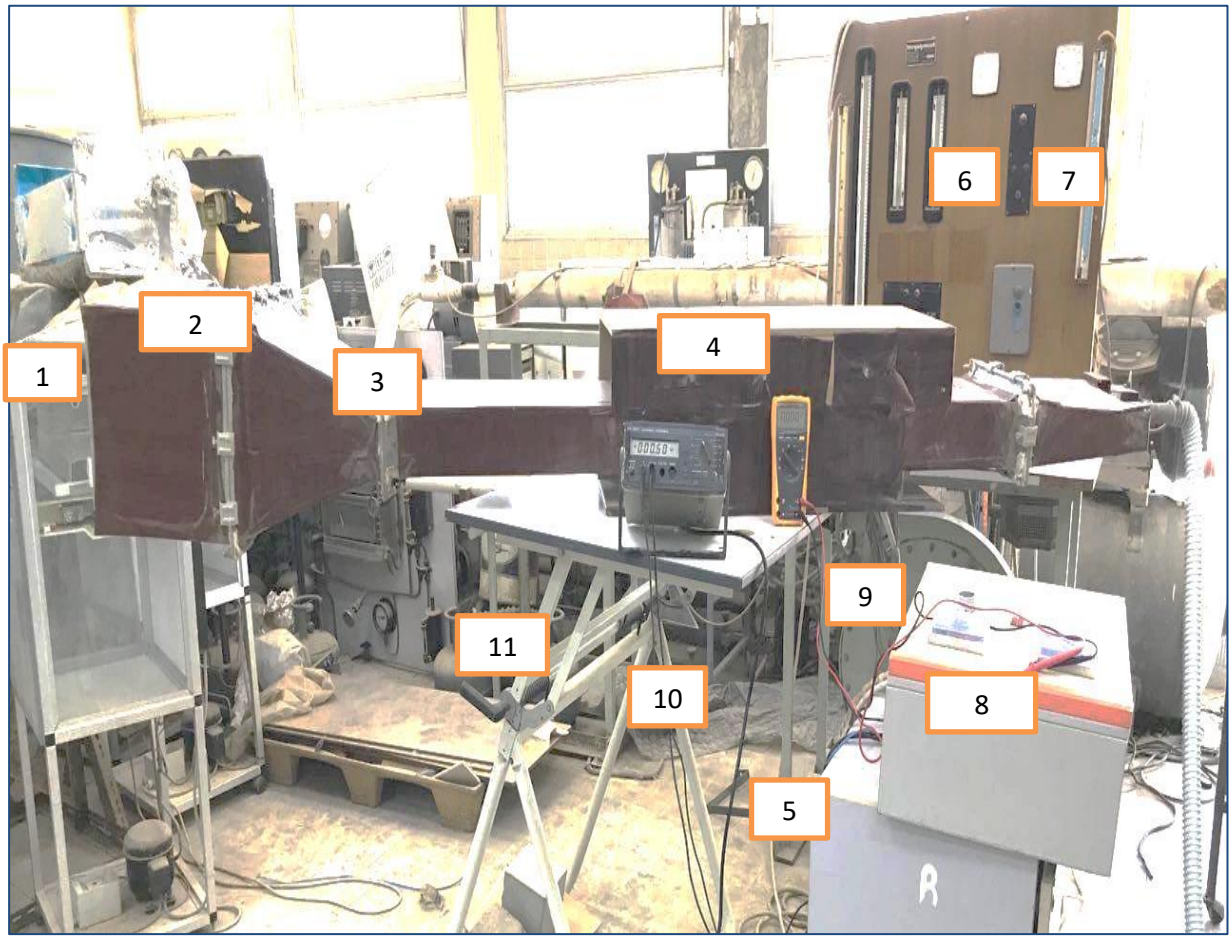

Figure 3. Photograph view of the components of the experimental rig; 1- Inlet air 2- Damping Chamber 3- Inlet nozzle 4- Test section 5- Fan 6- Ammeter 7- Voltmeter 8- Selector switch 9- True-rms multimeter 10- Automatic multimeter 11- Wooden board.

3. Experimental variables analysis.

The data obtained during the present test work as values of voltage and electric current then the temperature and velocity are recorded at transfer from the hot base(bottom plate) and array fins by convection are determined by applying an energy balance [5],

$$Q_{convection}=Q_{total} - Q_{conduction}-Q_{radiation} \quad (1)$$

Where Q_{total} is total dissipated energy from the surface heater source, $Q_{conduction}$ is the total loss of heat conduction across the insulation and $Q_{radiation}$ is the total loss of heat radiation from hot base and (finned wall) surface [6]. The total energy dissipated as below.

$$Q_{tota}=V.I \quad (2)$$

The voltage drop V and the current I are measured during experimental. The conduction heat loss through the insulation of the test section was calculated from:

$$Q_{conduction}=-K_{insulation}A_{insulation}\frac{\Delta T_{insulation}}{L_{insulation}} \quad (3)$$

Where: $K_{insulation}$ is the insulation thermal conductivity. ΔT is the difference surface temperature of the insulation. The heat removed by radiation can be the assumption of diffuse, opaque isothermal and gray surface [6]:

$$Q_{radiation}=\varepsilon F A_R \sigma(T_w^4-T_b^4) \quad (4)$$

Where: (*F*) is the shape factor of gray body, (A_R) is the surface area for radiation heat transfer, and (σ) Stephan –Boltzmann constant 5.67×10^{-8} W/m^2.K^4.

The dimensionless number that affected on the heat transfer were,

i-The Reynolds number:

$$Re=\frac{w_{in}D_h}{\nu_{air}} \quad (5)$$

$$D_h=\frac{4A_c}{P_c} \quad (6)$$

ii-The modified Grashof number Gr^*:

$$Gr^*=\frac{g\,\beta q''_{con} D_h{}^4}{k_{air}\nu_{air}{}^2} \quad (7)$$

Where: $q''_{con}=\frac{Q_{convection}}{A_b}$ is average flux heat convection transfer to the air. A_c is the cross-section area of channel and P is the perimeter of the channel.

iv-Average heat transfer coefficient h_{av}:

The average heat coefficient for the heated plate as:

$$h_{av}=\frac{Q_{convection}}{A_b(T_{w_{av}}-\frac{T_w+T_{air}}{2})} \quad (8)$$

Where $Q_{convection}$ is convection heat transfer rate to the fluid. A_b=L*W is un finned heated plate. T_w and T_{air} are average temperatures of the surface plate and baulk temperature.

air ($\frac{T_{out}+T_{in}}{2}$). The properties of air are determined at the average of the plate and air inlet temperature ($\frac{T_{w_{av}}+T_{air}}{2}$).

iiv-Overall effectiveness of fin arrays [4]:

These can be listed as follows:

$$\varepsilon_f=\frac{(Q_{unfin}+n_f Q_{fin})}{Q_{nofin}} \quad (9)$$

$$Q_{unfin}=h_{av}A_{\text{unfin}}(T_{w_{av}}-T_{air}) \quad (9a)$$

$$Q_{fin}=h_{av}A_{\text{fin}}(T_{w_{av}}-T_{air})\eta_f \quad (9b)$$

$$Q_{nofin}=h_{av}A_{\ nofin}(T_{w_{av}}-T_{air}) \quad (9c)$$

$$A_{\text{fin}}=2\times H_f\times L_f+(L_f\times t) \quad (10a)$$

$$A_{\text{unfin}}=w\times L_f-n_f(t\times L_f) \quad (10b)$$

$$A_{\ nofin}=w\times L_f \quad (10c)$$

4. Results and discussion.

Experimental data used in performance analysis were obtained for the fin arrays of material aluminium, in the two-dimensional hot base channel.

4.1 Effect of Grashof Number

Figure 4presentsthe variation of local base temperature along with the distance all the length of hot base section θ = 150, Reynolds number =2300, and with variable (Gr^*). It can be observed from this figure, that the local temperature values in the entry of the test section at z = 0m have nearly same inlet temperature then, the temperature will increases until reaches a maximum value at z = 0.4 m due to buoyancy force.

The variation of local heat transfer coefficient at θ = 150, Re = 2300 and different (Gr^*)are illustrated in figure 5. In the access region of the test section force, convection features seem clear on behavior the heat transfer coefficient. The buoyancy forces become strong to destabilize the boundary layer so as a result inhibits the drop in local heat transfer coefficient. It can be seen from these figures. The h_z increases with Gr^*.

The variation of the average heat transfer coefficient with Reynolds number for various orientation angles and various values of Gr^* is explained in Figure 6.. The result obtained show that the average heat transfer coefficient increased with Grashof number for all orientation angles because the buoyant force is working in the direction of flow which developed with higher orientation angle. Moreover, at low Grashof number heat transfer is predominated by force convection while as Grashof number increase the heat transfer will accrue due to the start of secondary flow.

4.2Effect of inclination angles.

Figures 7 and 8 explain the influence of duct inclination on the thermal performance of the local surface temperature and heat transfer coefficient at Re = 2000 and $Gr^*=5\times10^8$. The plots show that the variation of both T_{wz} and h_z along the duct, the wall is influenced by orientation angles. Highest T_{wz} will be at θ =180°, so heat transfer increases as compared with that in θ = 90° in the application of the Newtons cooling equation.

Figure 9 presents the average heat transfer coefficient distribution for different orientation angles and Gr^*. The result shows that with a low value of Gr^*, the orientation angles slightly impact on h_{av} compared with the high value of Gr^*. The accelerating of the flow and heat transfer further enhanced by heat flux, as well as with an increase in orientation angles.

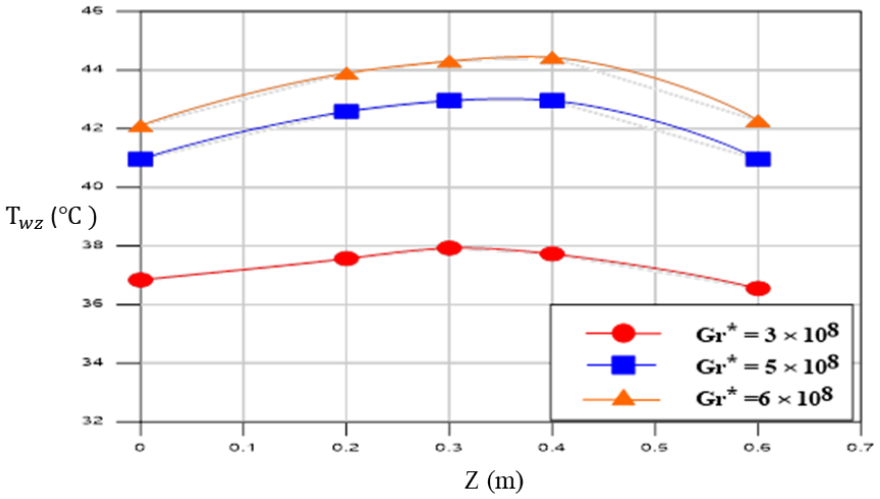

Figure 4. Variation of local base temperature for different Grashof number at orientation angle θ = 150º, Re = 2300.

4.3 Fin performance.

For evaluating the overall effectiveness of fin arrays are required to find out fins performance for different orientation angles (90°, 150°and 180°) and $Gr^*=5\times10^8$. Figure 10 illustrated the effect of these parameters on the fin effectiveness for different Reynolds number. Results show that with increasing Reynolds number, the fins effectiveness are decreased for all orientation angles also, but are

higher than the required value (2) as recorded by [7]. This means that the use of fin arrays at different orientation angles leads to an advantage based on heat transfer enhancement. It is clear that the overall effectiveness of fins (ε_f) are higher at θ = 180° than other angles.

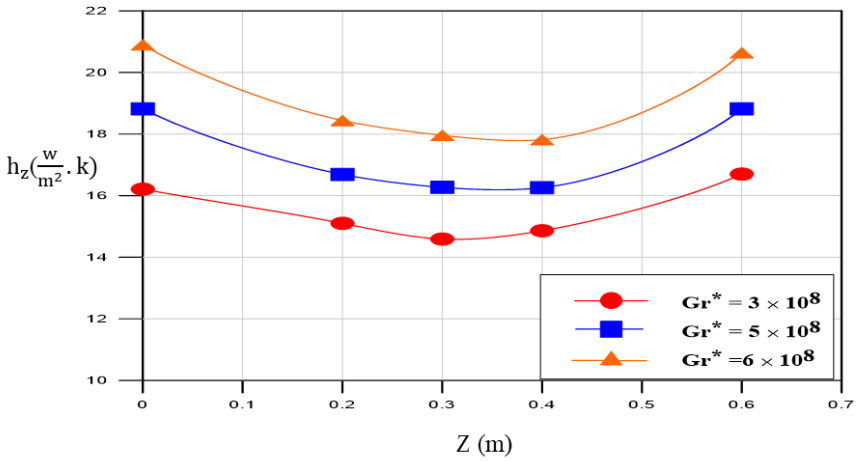

Figure 5. Variation of local heat transfer coefficient vs base length and constant orientation angle θ = 150°, Re = 2300.

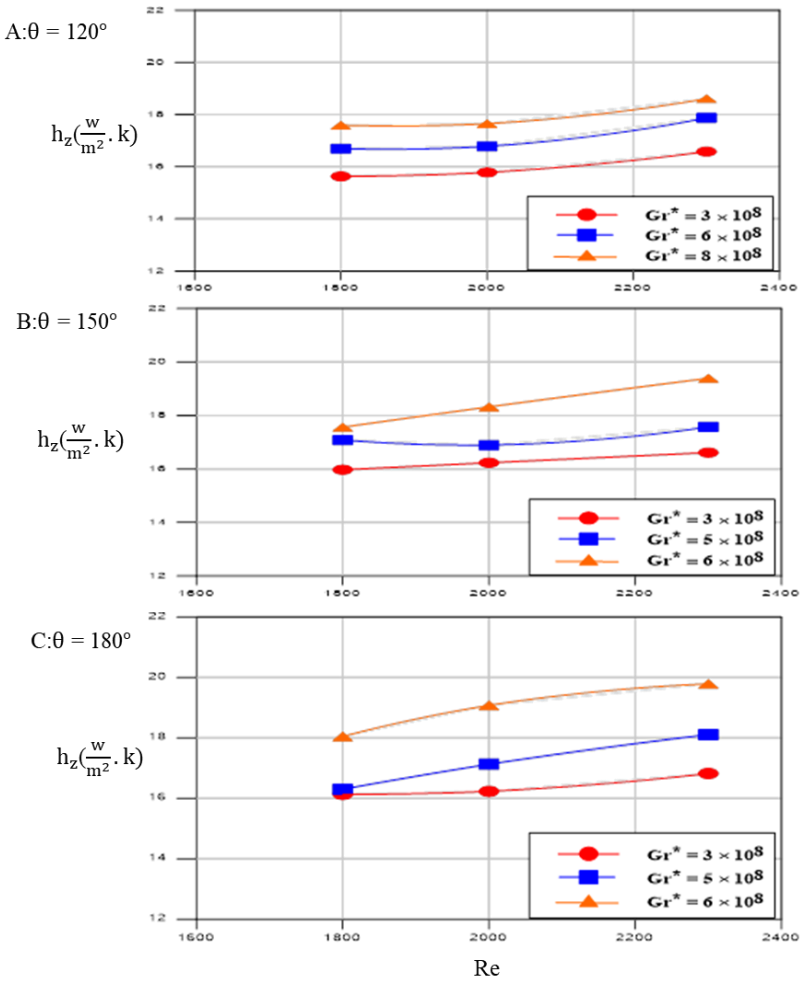

Figure 6. Average heat transfer coefficient versus Reynolds number and A, B & C orientation angles.

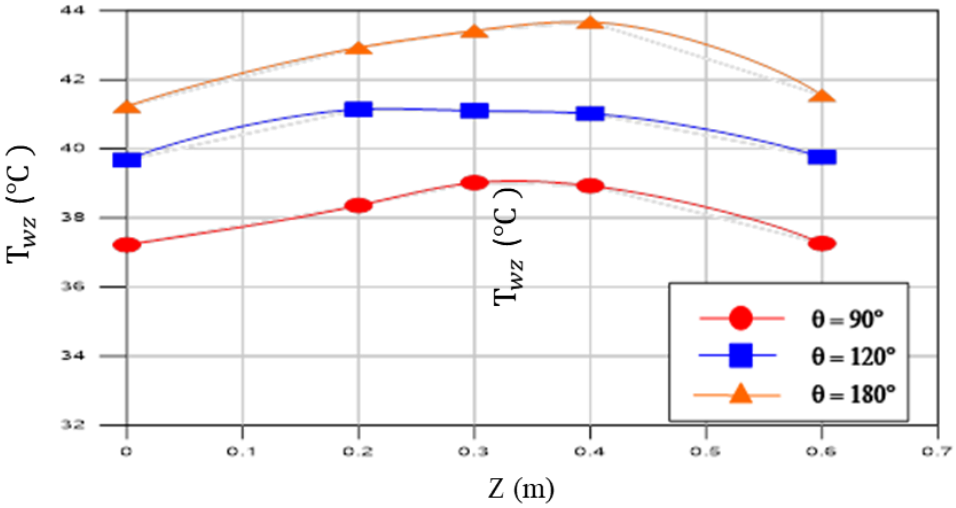

Figure 7. Variation of local base temperature for different orientation angles, $\mathrm{Re} = 2000$, $\mathrm{Gr}^{*} = 5 \times 10^{8}$.

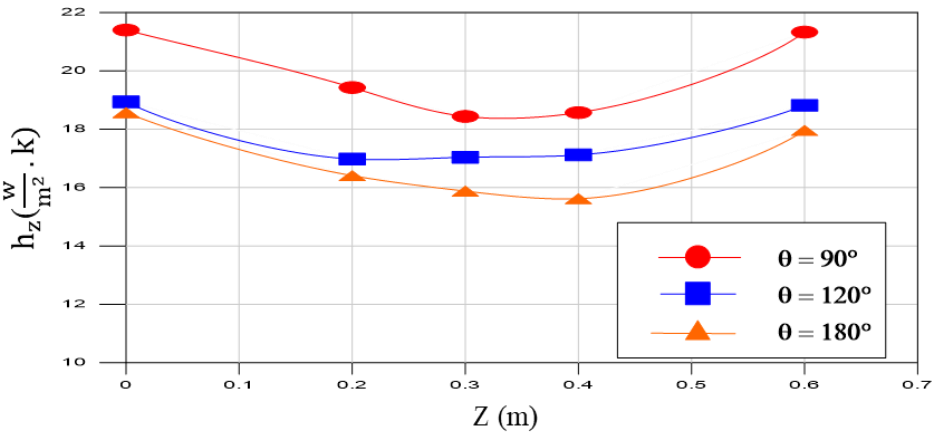

Figure 8. Variation of local heat transfer coefficient for different orientation angles, $\mathrm{Re} = 2000$, $\mathrm{Gr}^{*} = 5 \times 10^{8}$.

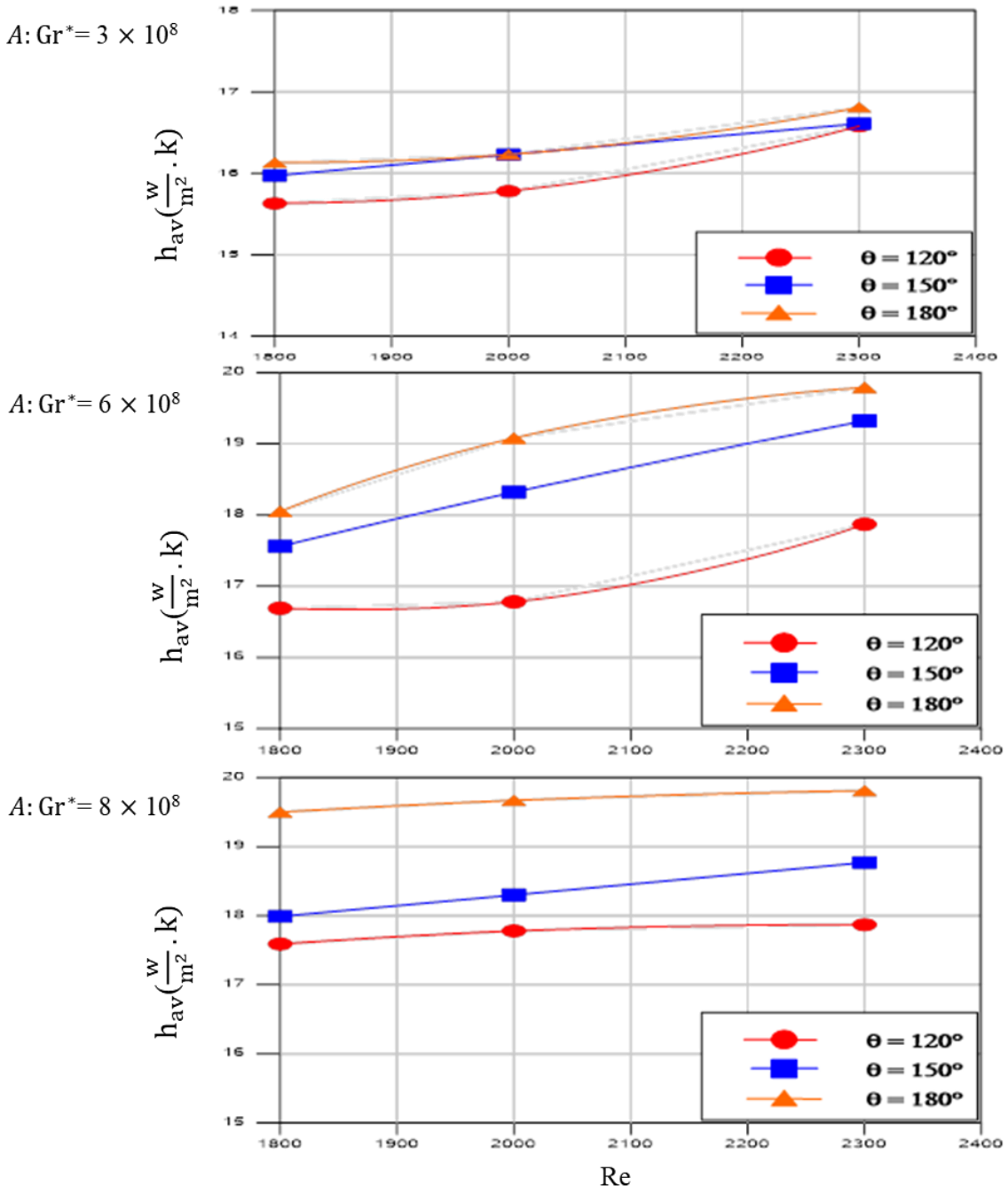

Figure 9. Average heat transfer coefficient vs Reynolds number, different orientation angles and A, B & Constant Gr*.

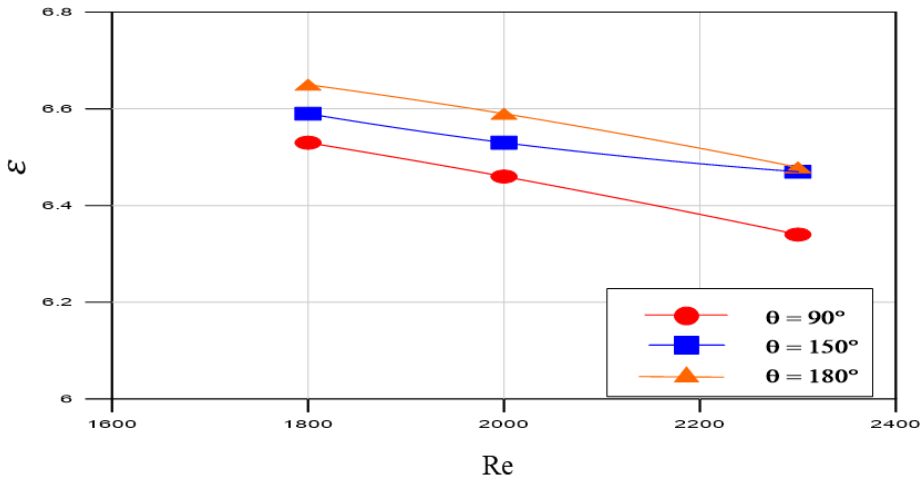

Figure 10. Fin performance vs Reynolds number for different orientation angles and, $Gr^{*}= 5 \times 10^{8}$.

5. Conclusions

From the experimental work, the following can be concluded:

- For all orientation angles, the removal heat increases when the Reynolds number and Grashof number are increasing.
- The higher Reynolds number, smaller fluctuation in the average heat transfer coefficient is observed due to forced convection.
- As orientation angles increasing, buoyancy effect increases thus which causes an unsteady movement flow.
- The average heat transfer coefficient and fins effectiveness are enhanced to 25% at highest longitudinal orientation angles

6. Nomenclature.

A_c: Channel cross section area (m2)
t : Thickness of fin (m)
H_f : Fin height (m)L_f : Length of fin (m)
w_{in} : Mean longitudinal velocity (m/s)
P: perimeter (m)
K_a : Thermal conductivity of air (W/m K)
N_p : Number of perforations
T_{in}: Inlet air Temperature (℃) $q^{"}$: Convection heat flux (W/m^2)
T_{out} : Outlet air Temperature (℃)
S: Fin spacing (m)
D_{h} : Hydraulic diameter of the duct (m)
Re: Reynolds number
h_{av} : Average Heat transfer coefficient (W/m^2. K)
Gr*: Modified Grashof number
ε_f: Overall effectiveness of fin arrays n_f: Number of fin
Q_{unfin}: Convection heat transfer from the surface between two fins.
Q_{fin}: Convection heat transfer from the fins.
Q_{nofin}: Convection heat transfer from the surface without any fins.
v: Kinematic viscosity of air (m^2/s)

β: Thermal expansion coefficient (1/k)

7-References.

[1] Uniyal M. and Joshi K., 2015 "Numerical and Experimental Investigation Plane Fin with the Help of Passive Augmentation Method*", IOSR Journal of Mechanical and Civil Engineering* (IOSR-JMCE), Vol. 12, Issue 6, Ver. II, PP 48-53.
[2] Webb L. R., "Principles of Enhanced Heat Transfer", *Second Edition, Taylor & Francis Group*, New York, 2005.
[3] Park H. and Chung B., 2015 "Optimal tip clearance in the laminar forced convection heat transfer of a finned plate in a square duct", *International Communications in Heat and Mass Transfer*,.
[4] Cengel, Y.A., 2002"*Heat Transfer", a Practical Approach*, 2nd.Edition,.
[5] Tahat M., Kodah Z.H., Jarrah B. A. and Probert S. D., 2000"Heat transfers from pin-fin arrays experiencing forced convection", *Applied Energy* 67, pp. 419-442,.
[6] Al-Sarkhi A., Abu-Nada E., 2005 "Characteristics of forced convection heat transfer in vertical internally finned tube", *International Communications in Heat and Mass Transfe*r, 32, pp. 557–564,.
[7] Dogan M. and Sivrioglu M., 2010 "Experimental investigation of mixed convection heat transfer from longitudinal fins in a horizontal rectangular channel", *International Journal of Heat and Mass Transfer*, 53, pp. 2149-2158,